arXiv:astro-ph/0308206v2 6 Oct 2003

NEAR-INFRARED COLORS OF GAMMA-RAY BURST AFTERGLOWS AND COSMIC REIONIZATION HISTORY

Akio K. Inoue[1], Ryo Yamazaki[1], and Takashi Nakamura
Department of Physics, Kyoto University, Kyoto 606-8502, Japan
akinoue@tap.scphys.kyoto-u.ac.jp, yamazaki@tap.scphys.kyoto-u.ac.jp, takashi@tap.scphys.kyoto-u.ac.jp
submitted to ApJ

ABSTRACT

Using the near-infrared (NIR) observations of the afterglows of the high redshift ($5 \lesssim z \lesssim 25$) gamma-ray bursts (GRBs) that will be detected by the *Swift* satellite, we discuss a way to study the cosmic reionization history. In principle the details of the cosmic reionization history are well imprinted in the NIR spectra of the GRB afterglows. However the spectroscopy with a space telescope is required to obtain such an information for a very high redshift ($z \gtrsim 15$) unless the neutral fraction of the high-z universe is less than 10^{-6}. The broad-band photometry has the higher sensitivity than that of the spectroscopy, so that the NIR photometric follow-up of the GRB afterglows is very promising to examine the cosmic reionization history. A few minutes exposure with a 8-m class ground-based telescope of the afterglow of the high-z GRBs will reveal how many times the reionization occurred in the universe.

Subject headings: cosmology: observations — gamma rays: bursts — intergalactic medium — radiative transfer — techniques: photometric

1. INTRODUCTION

The evolutionary study of the intergalactic medium (IGM) is now one of the most active fields in astrophysics. Especially, the cosmic reionization history of the IGM attracts many researchers in recent years (see Loeb & Barkana 2001 for a review). Gunn–Peterson trough shortward of the Lyα resonance (Gunn & Peterson 1965) in the spectrum of quasars with redshift $z \sim 6$ indicates that the end of the reionization epoch is $z \sim 6$ (Becker et al. 2001; White et al. 2003). On the other hand, the recent observation of the polarization of the cosmic microwave background (CMB) by *WMAP* suggests that the beginning of the reionization is $z \sim 20$ (Spergel et al. 2003; Kogut et al. 2003). One might think that there is a discrepancy between both observations.

The detailed simulation of the six-dimensional radiative transfer shows that the reionization process proceeds slowly in an inhomogeneous universe (e.g., Nakamoto, Umemura, & Susa 2001). If the reionization began at $z \sim 20$, the neutral fraction in the universe decreased gradually, and the universe was ionized almost completely at $z \sim 6$, the apparent discrepancy can be resolved (Wyithe & Loeb 2003a; Haiman & Holder 2003; Ciardi, Ferrara, & White 2003; Chiu, Fan, & Ostriker 2003; Sokasian et al. 2003; Onken & Miralda-Escudé 2003). The scenario that the initial partially ionized epoch was simply followed by the complete ionization can explain the large Thomson scattering opacity observed from the CMB polarization and also is consistent with the previous picture in which the end of the reionization is $z \sim 6$.

Cen (2003a,b) and Wyithe & Loeb (2003b) recently proposed a new scenario of the reionization; the universe was reionized twice. Even in an inhomogeneous universe, enough strong intensity of the ultra-violet (UV) background radiation can ionize the universe quickly. At $z \sim 20$, the first reionization was made by the Population

III (Pop III) stars (metal-free stars) with a top-heavy initial mass function (IMF) which yields a much higher UV emissivity than that of normal Pop I and II stars. Then, the universe was partially recombined at $z \sim 15$ when the transition from the Pop III to II was occurred and the UV emissivity was suddenly suppressed because of the different IMF. Finally, the UV photons from the Pop II stars increased gradually and ionized the universe again at $z \sim 6$.

Cen's scenario can also resolve the discrepancy, but it is different from others in the history of the cosmic reionization; the first complete ionization was followed by the partially ionized epoch and then the second complete ionization. We should assess whether Cen's scenario is favored by using other observations. In this paper, an assessment by using the afterglows of the gamma-ray bursts (GRBs) is discussed.

The usefulness of GRBs to investigate the high-z universe is pointed out by many authors (e.g., Lamb & Reichart 2000; Ciardi & Loeb 2000; Barkana & Loeb 2003). It is strongly suggested that the long duration GRBs arise from the collapse of a massive star (Galama et al. 1998; Uemura et al. 2003; Hjorth et al. 2003; Price et al. 2003; Stanek et al. 2003; Matheson et al. 2003). Hence, the GRBs can occur at very high-z once the massive stars are formed. For example, the *Swift* satellite[2] is expected to detect ~ 10 GRBs per year occurring at $z \gtrsim 10$ (Lamb & Reichart 2000). Furthermore, if we fix an observing time from the prompt emission, the observed afterglow flux does not become so faint even for the extremely high-z GRBs because the earlier phase of the afterglow is observed in the cosmological rest frame (Ciardi & Loeb 2000).

In this paper, we show that the near-infrared (NIR) photometric follow-ups of the GRB afterglows are very useful to investigate how many times the cosmic reionization occurred. Although many techniques to prove the reioniza-

---

tion history have been proposed so far, for example, hydrogen 21 cm line tomography (Madau, Meiksin, & Rees 1997; Carilli, Gnedin, & Owen 2002; Furlanetto & Loeb 2002), Lyα damping wing measurement (Miralda-Escudé 1998; Barkana & Loeb 2003), metal absorption lines (Oh 2002; Furlanetto & Loeb 2003), CMB polarization anisotropy (Haiman & Holder 2003), and dispersion measure in GRB radio afterglows (Ioka 2003; Inoue 2003), the NIR photometric colors may be the most promising technique using the *current* facilities.

In order to investigate the reionization history using our photometric method, we need to determine redshifts of GRBs by other ways, e.g., detections of iron lines in X-ray afterglow spectra (Mészáros & Rees 2003) and of the Lyα break in NIR spectra, or empirical methods by using only the γ-ray data (Fenimore & Ramirez-Ruiz 2000; Norris et al. 2000; Ioka & Nakamura 2001; Amati et al. 2002; Atteia 2003; Murakami et al. 2003; Yonetoku et al. 2003). Even if redshifts of GRBs are unknown prior to follow-up observations, it is worth performing NIR photometry as early phase as possible since $\sim 10\%$ of GRBs are expected to be located at $z \gtrsim 10$ (Bromm & Loeb 2002). In practice, such follow-up observations against every GRB are possible. Even after the early NIR follow-up, we will be able to determine the redshifts. In this paper, we show that the near-infrared (NIR) photometric follow-ups of the GRB afterglows provide a significantly important information on the cosmic reionization history.

The structure of this paper is as follows: we start from a brief summary of the IGM opacity by the neutral hydrogen in section 2. In section 3, the possible scenario of a very low neutral fraction at very high-z is discussed. Then, we examine the NIR spectra and colors of the GRB afterglows in section 4 and 5, respectively. Finally, we discuss a way to obtain the cosmic reionization history and advantage/disadvantage of our method in section 6.

We adopt a standard set of the ΛCDM cosmology throughout the paper: $H_0 = 70$ km s^{-1} Mpc^{-1}, $\Omega_{\rm M} = 0.3$, $\Omega_\Lambda = 0.7$, and $\Omega_{\rm b} = 0.04$.

2. IGM OPACITY

Suppose an observer at $z = 0$ who observes a source with $z = z_{\rm S}$ at the observer's frequency ν_0. The radiation from the source is absorbed by the Lyman series lines and the photoionization of the intervening neutral hydrogen (Gunn & Peterson 1965). The hydrogen cross section at the rest frame frequency ν is

$$\sigma_{\rm HI}(\nu) = \sigma_{\rm LC}(\nu) + \sum_i \sigma_i(\nu) \,, \qquad (1)$$

where $\sigma_{\rm LC}(\nu)$ is the cross section for the Lyman continuum photons ($h\nu \geq 13.6$ eV) and $\sigma_i(\nu)$ is the cross section for the i-th line of the Lyman series, i.e., $i =$ Lyα, Lyβ, Lyγ, etc. Here we consider the lines up to $i = 40$. The optical depth for the observer's frequency ν_0 is given by

$$\tau_{\nu_0}(z_{\rm S}) = \tau_{\nu_0}^{\rm LC}(z_{\rm S}) + \sum_i \tau_{\nu_0}^i(z_{\rm S}) \,, \qquad (2)$$

$$\tau_{\nu_0}^{\rm LC}(z_{\rm S}) = \int_0^{z_{\rm S}} \sigma_{\rm LC}(\nu_0[1+z]) n_{\rm HI}(z) \frac{c\,dz}{(1+z)H(z)} \,, \qquad (3)$$

and

$$\tau_{\nu_0}^i(z_{\rm S}) = \int_0^{z_{\rm S}} \sigma_i(\nu_0[1+z]) n_{\rm HI}(z) \frac{c\,dz}{(1+z)H(z)} \,, \qquad (4)$$

where $n_{\rm HI}(z)$ is the number density of the neutral hydrogen at the redshift z, $H(z)$ is the Hubble constant at the redshift z, and c is the light speed.

The cross section for the Lyman continuum photons is given by $\sigma_{\rm LC}(\nu) = \sigma_{\rm L}(\nu/\nu_{\rm L})^{-3}$, where $\sigma_{\rm L} = 6.30 \times 10^{-18}$ cm^2 and the Lyman limit frequency $\nu_{\rm L} = 3.29 \times 10^{15}$ Hz (Osterbrock 1989). Thus, we obtain

$$\tau_{\nu_0}^{\rm LC}(z_{\rm S}) = \sigma_{\rm L} \left(\frac{\nu_{\rm L}}{\nu_0}\right)^3 n_{\rm H,0} c \int_{z_{\rm min}}^{z_{\rm S}} \frac{x_{\rm HI}(z)dz}{(1+z)H(z)} \,, \qquad (5)$$

where $x_{\rm HI}(z)$ is the neutral fraction at the redshift z and $z_{\rm min} = \max[0, (\nu_{\rm L}/\nu_0) - 1]$. The neutral fraction $x_{\rm HI}(z)$ is defined as $n_{\rm HI}(z)/n_{\rm H}(z)$, where $n_{\rm H}(z) = n_{\rm H,0}(1+z)^3$ is the cosmic mean number density of hydrogen atom at the redshift z with $n_{\rm H,0}$ being the present one. The effect of the inhomogeneity of the universe can be expressed in the definition of $x_{\rm HI}$ (see section 3 below). Since we need the condition $z_{\rm min} < z_{\rm S}$ to integrate Eq. (5), $\tau_{\nu_0}^{\rm LC}(z_{\rm S}) = 0$ when $\nu_0 \leq \nu_{\rm L}/(1+z_{\rm S})$.

The line cross section $\sigma_i(\nu)$ has a very sharp peak at the line center frequency. The width is well characterized by the Doppler width, $\Delta\nu_{\rm D}$. That is, $\sigma_i(\nu) \simeq \sigma_i$ for $|\nu - \nu_i| \leq \Delta\nu_{\rm D}$, and $\sigma_i(\nu) \simeq 0$ for $|\nu - \nu_i| > \Delta\nu_{\rm D}$, where σ_i and ν_i are the cross section and the frequency of the i-th line center, respectively. Since $\nu = \nu_0(1+z)$, we integrate the rhs of equation (4) over a narrow redshift width of $\Delta(1+z) = 2(\Delta\nu_{\rm D}/\nu_i)(1+z_i)$ around $1+z_i = \nu_i/\nu_0$. Therefore, we obtain

$$\tau_{\nu_0}^i(z_{\rm S}) \simeq 2 \left[\frac{\sqrt{\pi}e^2 f_i}{m_e c \nu_i}\right] \left[\frac{c n_{\rm HI}(z_i)}{H(z_i)}\right] \,, \qquad (6)$$

where we have substituted $\sigma_i = \sqrt{\pi}e^2 f_i/m_e c\Delta\nu_{\rm D}$, in which e is the electric charge, f_i is the absorption oscillator strength of the i-th line, and m_e is the electron mass. The values of f_i and ν_i are taken from Wiese, Smith, & Glennon (1966). This time also we are restricted by $z_i \leq z_{\rm S}$. Thus, the above equation is valid only when $\nu_0 \geq \nu_i/(1+z_{\rm S})$, otherwise $\tau_{\nu_0}^i(z_{\rm S}) = 0$.

For the Lyα line, the opacity becomes

$$\tau^{\rm Ly\alpha} \simeq 2.6 \times 10^6 x_{\rm HI}(z) \left(\frac{1+z}{20}\right)^{3/2} \,, \qquad (7)$$

where we approximate $H(z) \approx H_0\Omega_{\rm M}^{1/2}(1+z)^{3/2}$ and adopt $n_{\rm HI}(z) = x_{\rm HI}(z)n_{\rm H,0}(1+z)^3$. This is the Gunn-Peterson optical depth (Gunn & Peterson 1965; Peebles 1993). From this equation, we realize that if $x_{\rm HI} \gtrsim 10^{-6}$, the IGM is opaque for the photon bluer than the source Lyα line. Conversely, we can estimate $x_{\rm HI}$ if $\tau^{\rm Ly\alpha}$ is determined observationally (e.g., Becker et al. 2001; White et al. 2003).

3. NEUTRAL FRACTION AND STAR FORMATION RATE

In the following sections, we will assume a neutral fraction of hydrogen, $x_{\rm HI} \sim 10^{-6}$ at $z \sim 20$ for calculations of spectra and colors of GRB afterglows. Before such calculations, we show, here, that $x_{\rm HI} \sim 10^{-6}$ is possible at a very high-z universe.[3]

---

[3] In Figure 9 of Cen (2003a), the neutral fraction decreases up to 10^{-4}. However, it is an artificial limit in his calculation (Cen 2003, private communication).

In general, the neutral fraction, $x_{HI}(z)$, is spatially variable. However, we discuss only its mean value for simplicity. The averaged x_{HI} is determined by the UV intensity of the background radiation and the inhomogeneity of the hydrogen number density at the redshift z. Even at very high-z universe, the recombination time-scale is much less than the Hubble time-scale. Thus, we assume the ionization equilibrium. In that case, the mean neutral fraction for a highly ionized medium (i.e. $x_{HI} \ll 1$) is given by $x_{HI} \approx Cn_H\alpha/\Gamma_{HI}$, where $C = \langle n_H^2 \rangle/\langle n_H \rangle^2$ is the clumping factor, n_H is the number density of hydrogen nuclei, α is the recombination coefficient, and $\Gamma_{HI} = \int \sigma_{LC}(\nu)cn_\nu d\nu$ is the HI photoionization rate where n_ν is the photon number density per frequency. Therefore, the UV background intensity is required to estimate x_{HI} even if we know the clumping factor from the model of the cosmological structure formation.

How much photons are required to control the hydrogen neutral fraction in a very low level? Approximately, the HI photoionization rate is estimated to be $\Gamma_{HI} \sim \sigma_L cn_{ion}$ with n_{ion} being the number density of ionizing photons. Hence, we find

$$\frac{n_{ion}}{n_H} \sim \frac{C\alpha}{\sigma_L c x_{HI}} \sim C\left(\frac{10^{-6}}{x_{HI}}\right), \qquad (8)$$

where the case B recombination rate $\alpha = 2.73 \times 10^{-13}$ cm^3 s^{-1} is adopted (Osterbrock 1989). Now, we are interested in a very high redshift universe ($z \sim 20$). In there, the clumping factor is an order of unity. Therefore, we find that only one photon per a hydrogen nuclei is sufficient to keep $x_{HI} \sim 10^{-6}$.

Then, we examine how much stars are required to maintain the photon density. Since a proton recombines with an electron in a certain time-scale, continuous supply of ionizing photons is needed to keep $n_{ion} \sim n_H$. Since the recombination time-scale is $\sim 1/n_H\alpha$ for $x_{HI} \ll 1$, the required photon emissivity per unit volume is estimated to be $\epsilon_{ion} \sim n_{ion}n_H\alpha \sim Cn_H^2\alpha^2/x_{HI}\sigma_L c$. On the other hand, the emissivity is given by $\epsilon_{ion} = f_{esc}\epsilon_{LC}\rho_{SFR}(1+z)^3$, where f_{esc} is the escape fraction of Lyman continuum from primordial galaxies, ϵ_{LC} is the Lyman continuum photon emissivity per unit stellar mass, and ρ_{SFR} is the star formation density per unit time per unit comoving volume. Therefore, the required star formation density is

$$\frac{\rho_{SFR}}{M_\odot \, yr^{-1} \, Mpc^{-3}} \sim 0.1C\left(\frac{0.1}{f_{esc}}\right)\left(\frac{10^{61} \, ph \, M_\odot^{-1}}{\epsilon_{LC}}\right)$$
$$\left(\frac{10^{-6}}{x_{HI}}\right)\left(\frac{1+z}{20}\right)^3. \qquad (9)$$

Although the photon emissivity at high-z is very uncertain because we don't know the stellar mass distribution, we estimate the emissivity by Starburst 99 model (Leitherer et al. 1999)[4] by assuming the Salpeter mass function with various mass ranges. The estimated values of ϵ_{LC} are summarized in Table 1. The Pop III stars are likely to have a top-heavy mass function (e.g., Nakamura & Umemura 2001). Hence, the case of 10–100 $M_\odot$ in Table 1 may be suitable. In this case, the required star formation density to maintain $x_{HI} \sim 10^{-6}$ is ~ 0.05 $M_\odot$ yr^{-1} Mpc^{-3} (comoving) when $f_{esc} = 0.1$ and $C = 1$.

Is this star formation density possible? The latest observations suggest that the star formation density retains

a level of ~ 0.1 $M_\odot$ yr^{-1} Mpc^{-3} from $z \sim 1$ to $z \sim 6$ (Giavalisco et al. 2003). Such a level of star formation may be kept toward more high-z universe. Moreover, a semianalytic model shows 0.01–0.1 $M_\odot$ yr^{-1} Mpc^{-3} at $z \sim 20$ depending on the assumed star formation efficiency (Somerville & Livio 2003). Thus, we can sufficiently expect ~ 0.05 $M_\odot$ yr^{-1} Mpc^{-3}, and then, $x_{HI} \sim 10^{-6}$ at $z \sim 20$. In addition, we note that the escape fraction may be much larger than 0.1 assumed above if the Pop III stars are formed in low-mass halos.

4. NEAR INFRARED SPECTRA

Let us discuss the observed spectra of the GRB afterglows in the NIR bands. To do so, an afterglow spectral model is required. We adopt a simple afterglow model; the synchrotron radiation from the relativistic shock (Sari, Piran, & Narayan 1998). More specifically, we adopt equations (1)–(5) in Ciardi & Loeb (2000) who take into account the effect of the cosmological redshift. The adopted parameters are the magnetic energy fraction of $\epsilon_B = 0.1$, the electron energy fraction of $\epsilon_e = 0.2$, the spherical shock energy of $E = 10^{52}$ erg, the ambient gas number density of $n = 10$ cm^{-3}, and the power-law index of the electron energy distribution $p = 2.5$.

First we consider the observed afterglow spectra in the hypothetical perfectly neutral universe for comparison. In Figure 1, we show the expected afterglow spectra in the neutral universe observed 1 hour after the burst in the observer's frame. Due to the Lyα line absorption, the continuum bluer than the Lyα line in the source frame (the observed wavelength $0.1216[1+z_S]$ μm) is completely damped. Thus, we can find the Lyα break clearly. From the observed wavelength of the Lyα break, we can determine the redshift of the GRBs. If we observe the afterglow through a filter, the radiation from the source with the redshift higher than the characteristic redshift of the filter cannot be detected because of the Lyα break. For example, the effect starts from $z_S \simeq 8$ for the J-band and the source with $z_S \gtrsim 11$ cannot be seen through the filter, i.e. *J drop-out*. These characteristic redshifts are summarized in Table 2. However, we have a chance to see the source beyond the drop-out redshift if the universe is highly ionized as we will show later.

Next we examine what is observed if the very high-z universe is ionized completely as proposed by Cen (2003a,b). Let us set the neutral fraction, x_{HI}, of the universe in the redshift range $15 \leq z < 20$ to be very small and $x_{HI} \sim 1$ for $z < 15$ and $z \geq 20$. That is, we assume that the Pop III stars ionized the universe at $z = 20$ and the sudden change of the IMF due to the transition from the Pop III to II was occurred at $z = 15$. The neutral fraction is determined by the background UV intensity produced by the Pop III stars. However, the intensity is quite uncertain, so that we choose two cases as $x_{HI} = 10^{-6}$ and 10^{-7} for instance (see also Fig.5 in section 5). We will present a way to constrain x_{HI} from the observations later.

In Figure 2, we show the expected spectra of the GRB afterglows. The solid, short-dashed, long-dashed, dot-dashed, and dotted curves are the expected afterglow spec-

---

[4] http://www.stsci.edu/science/starburst99/

tra of the GRB at $z_S = 22$, 20, 18, 15, and 13, respectively. The observing time is assumed to be 1 hour after the prompt emission in the observer's frame. We find the clear Lyα breaks in the spectra. Since $x_{HI} = 10^{-6}$ (or 10^{-7}) at $15 \leq z < 20$ is assumed in the panel (a) (or (b)), the IGM opacity is an order of unity (or 0.1) in the redshift range (see eq.[7]). Thus, the continuum bluer than the Lyα break of the GRBs with $z_S > 15$ still remains of the order of 10 μJy (or 100 μJy) in $\sim$ 2–2.5 μm, i.e.,in K-band (see the thin solid curve indicated as K; we adopt the filter system of Bessell & Brett 1988). The spectral break at 1.94(=0.1216[1+15]) μm is due to the neutral hydrogen below $z = 15$. Thus, the continuum less than the break wavelength in the observer's frame from the $z_S \geq 15$ source is completely extinguished. The spectra of the source with $z_S < 15$ are the same as those shown in Figure 1. For $z_S = 22$ case, the spectrum shows the second break at 2.36(=0.1026[1+22]) μm. This is the Lyβ break due to the neutral hydrogen near the GRB. Here we have assumed $x_{HI} \sim 1$ for $z \geq 20$.

The structure corresponding to the reionization history appears in the spectra of the GRB afterglows as shown in Figure 2 (see also Haiman & Loeb 1999). If we could detect the continuum rising at 2.55(=0.1216[1+20]) μm in the spectrum of the GRB with $z_S = 22$, we would find the starting epoch of the first reionization as $z = 20$. On the other hand, the end of the first reionization, in other words, the transition epoch from the Pop III to II is realized from the spectral break at 1.94(=0.1216[1+15]) μm.

The suitable band to determine the ionization history depends on the redshift of the reionization epoch. From Figure 1 (see also Table 2), we find that the I, J, H, and K-band spectroscopies are suitable for the reionization epoch at $z \simeq 5$–7, 8–11, 11–14, and 15–20, respectively. In any case, observations to detect the spectral signatures in the NIR afterglow spectra of the GRBs are strongly encouraged. If x_{HI} is smaller than 10^{-6}, we can clearly see the difference from Fig. 1 and confirm the double reionization.

In the above discussion, we assumed $x_{HI} = 10^{-6}$ and 10^{-7}. Let us argue what will happen for different values of x_{HI}. If $x_{HI} \gtrsim 10^{-6}$, the remaining flux decreases exponentially because the IGM opacity becomes much larger than unity; for example, the flux is about 1 nJy for $x_{HI} = 6 \times 10^{-6}$, and about 1 pJy for $x_{HI} = 10^{-5}$. It is quite difficult to detect such a low-level flux.

5. NEAR INFRARED COLORS

The photometric observations are available easier than the spectroscopy. We examine the expected apparent NIR colors of the GRB afterglows. Although we can discuss the apparent magnitude of the afterglows in one photometric filter, their dispersion is very large because the luminosity of the afterglows depends on many uncertain parameters such as the jet opening angle, the ambient matter density, the magnetic energy fraction and the relativistic electron energy fraction. On the other hand, the dispersion of the apparent colors can be quite small because the color does not depend on the absolute luminosity but only the spectral shape which does not change significantly in the observed NIR bands.

The apparent magnitude[5] in a filter band denoted as i is defined by

$$m_i = -2.5 \log F_i/F_{i,0}, \qquad (10)$$

where $F_{i,0}$ is the zero point flux density of the filter and F_i is the mean flux density through the filter which is

$$F_i = \frac{\int T_{i,\nu} f_\nu e^{-\tau_\nu} d\nu}{\int T_{i,\nu} d\nu}, \qquad (11)$$

where $T_{i,\nu}$ is the transmission efficiency of the filter and $f_\nu e^{-\tau_\nu}$ is the flux density entering the filter. If there is no intervening absorber between the source and the telescope, $\tau_\nu = 0$.

The observed color between two filter bands, i and j (the filter i is bluer than the filter j), is given by

$$m_i - m_j = (m_i - m_j)^{int} + (\Delta m_i - \Delta m_j), \qquad (12)$$

where $(m_i - m_j)^{int}$ is the intrinsic color of the source, and Δm_i and Δm_j are the absorption amounts in the filters i and j, respectively. When we consider the NIR filter bands and high-z GRBs (for example $z = 15$), the intrinsic afterglow spectrum is predicted to be proportional to $\nu^{-1/2}$ from $\sim$ 1 minute to several hours after the burst occurrence and proportional to $\nu^{-p/2}$ for later time in the standard afterglow model (Sari, Piran, & Narayan 1998; Ciardi & Loeb 2000). Other parameters adopted are described in the beginning of the section 3. In Table 3, we tabulate the intrinsic colors of the sources for the two cases of the spectral shape.

The absorption amount in the filter i is

$$\Delta m_i \equiv m_i - m_i^{int} = -2.5 \log \frac{\int T_{i,\nu} f_\nu e^{-\tau_\nu} d\nu}{\int T_{i,\nu} f_\nu d\nu}, \qquad (13)$$

where $m_i^{int} = m_i(\tau_\nu = 0)$ is the intrinsic (no absorption) apparent magnitude. In a certain band width $\Delta\nu$, the difference in the optical depth $\Delta\tau$ is estimated as $|\Delta\tau/\tau| = 3/2(1+z)^{-1}|\Delta(1+z)| \sim (1+z)^{-1}|\Delta\nu/\nu|$ from equation (7). Since $\Delta\nu$ of the filter transmission is smaller than the effective frequency of the filter, i.e. $\Delta\nu/\nu < 1$, and also $z \gtrsim 5$, $\Delta\tau/\tau \ll 1$, that is, the term $e^{-\tau_\nu}$ in the integral of the numerator in equation (13) can be regarded as almost constant. Hence, we obtain approximately $\Delta m_i \approx 1.086\tau_{eff}$, where τ_{eff} is the effective IGM opacity in the filter i.

Now we can estimate the observed color by equation (12) if Δm_i is known. To know Δm_i is equivalent to know the IGM effective opacity τ_{eff}. This opacity is one between the redshift at which the Lyα break comes into the filter band width ($z_{Ly\alpha,in}^i$, see Table 2) and the source redshift (z_S) because the neutral hydrogen in $z < z_{Ly\alpha,in}^i$ cannot absorb the photons passing through the filter i. We note that the neutral hydrogen lying beyond the redshift at which the Lyα break goes out of the filter band width ($z_{Ly\alpha,out}^i$, see Table 2) absorb the photons through the filter i because of the higher-order Lyman series lines like Lyβ, Lyγ, etc., and the photoionization process. As a result, τ_{eff} is determined by the neutral fraction x_{HI} in the redshift range $z_{Ly\alpha,in}^i \leq z \leq z_S$. Since x_{HI} at high-z is uncertain, we assume that x_{HI} is constant in the above range for simplicity. The real x_{HI} might vary significantly in the redshift range,

---

[5] All magnitudes in this paper are the Vega system.

so that the assumed $x_{\rm HI}$ should be regarded as an effective mean value including such a variation (hereafter $x_{\rm HI}^{\rm eff}$).

In Figures 3a–3d, we show Δm_i for the I, J, H, and K-bands as a function of the source redshift. The continuum in the observer's L-band is not absorbed by the IGM neutral hydrogen at all when the source redshift is less than about 25. Although we assumed that the spectral shape is proportional to $\nu^{-1/2}$ in the panels, the results are much robust for the change of the spectral shape as noted above. The solid curves in these panels are loci of Δm_i for a given $x_{\rm HI}^{\rm eff}$ as a function of the source redshift $z_{\rm S}$. For example, since $z_{\rm Ly\alpha,in}^{I} = 5$ for I-band, the IGM absorption in I-band is about 5 mag for the source at $z_{\rm S} = 7$ if the effective neutral fraction $x_{\rm HI}^{\rm eff}$ in the redshift range $5 \leq z \leq 7$ is 10^{-5}.

Two dotted vertical lines in each panel of Figure 3 indicate the redshifts when the Lyα break enters and goes out of the each band width ($z_{\rm Ly\alpha,in}^{i}$ and $z_{\rm Ly\alpha,out}^{i}$, respectively). As seen in Figure 1, if the IGM is significantly neutral, the source with $z_{\rm S} > z_{\rm Ly\alpha,out}^{i}$ cannot be detected through the filter i (i.e. *drop-out*). However, we can detect such a source if the universe is highly ionized. This is because the continuum below the Lyα break remains as shown in Figure 2.

Suppose we observe a source with $z_{\rm S} > z_{\rm Ly\alpha,out}^{i}$ through the i and j filters and assume that the radiation through j filter is not affected by any intervening absorption (i.e. $\Delta m_j = 0$). From equation (12), the expected magnitude through the i filter is

$$m_i = m_j + (m_i - m_j)^{\rm int} + \Delta m_i. \qquad (14)$$

For example, we consider the case of $i = I$, $j = L$, and $z_{\rm S} = 7$. We find that the apparent L magnitude of the afterglow of the GRB at $z_{\rm S} = 7$ for 1 hour after the prompt burst is about 14 mag from Figure 4. Thus, the apparent I magnitude is expected to be 22 mag because the intrinsic $I - L = 3.1$ mag for 1 hour (i.e. the case $\propto \nu^{-1/2}$ in Table 3) and $\Delta I \sim 5$ mag if $x_{\rm HI}^{\rm eff} = 10^{-5}$ in the redshift range $5 \leq z \leq 7$. We can reach 5-σ detection of the source with $I = 22$ mag by only three minutes exposure with a 8-m class telescope. Interestingly the assumed $x_{\rm HI}^{\rm eff}$ is similar to the value reported by White et al. (2003) from the Gunn–Peterson trough in the spectra of $z > 6$ quasars.

Similar argument can be done for other bands. Therefore, in general, the detection of the source with $z_{\rm S} > z_{\rm Ly\alpha,out}^{i}$ through the filter i is the very good evidence that the universe in the redshift range $z_{\rm Ly\alpha,in}^{i} \lesssim z \lesssim z_{\rm S}$ is highly ionized, i.e. $x_{\rm HI}^{\rm eff} \ll 1$ in that redshift range. Conversely, the detection enables us to estimate $\tau_{\rm eff}$ and $x_{\rm HI}^{\rm eff}$. Finally, we note here that Figure 3 is also useful for any other sources (e.g., QSOs) because Δm_i is almost independent of the source spectrum.

6. DISCUSSIONS

6.1. *Was the universe reionized twice?*

Here we discuss how we can confirm or refute Cen's scenario: the universe was reionized twice. In the scenario, the first complete ionization at $z \sim 20$ is followed by the partially ionized epoch at $z \sim 10$. Therefore, we should check whether the neutral fraction at $z \sim 20$ is very low or not and whether the fraction at $z \sim 10$ is almost unity

or not. To do so, the best observation is the spectroscopy in the NIR bands. As shown in Fig. 2 of section 3, the reionization history is imprinted in the observed continuum. However, the sensitivity of the spectroscopy is in general much less than that of the photometric observations. Hence we discuss the way using the NIR photometries.

In the previous section, we have shown that the detection of the GRB afterglows through a filter i beyond the Lyα drop-out redshift ($z_{\rm Ly\alpha,out}^{i}$) proves the ionization of the universe around $z_{\rm Ly\alpha,out}^{i}$. From the characteristic redshifts for the NIR filters summarized in Table 2, the I, J, H, and K filters are the suitable to check the ionization state at $z \sim 5$–8, 8–11, 11–15, and 15–20, respectively. Thus, the null detection of the GRB afterglows of $z_{\rm S} \sim 11$ in J-band indicates an high neutral fraction in $8 \lesssim z \lesssim 11$. On the other hand, we detect the GRB afterglows of $z_{\rm S} \sim 20$ in K-band if the IGM in $15 \lesssim z \lesssim 20$ is ionized. I and H-band surveys are also very important to assess the reionization history of the universe. We can constrain the latest reionization epoch by observing the GRB afterglows at $z \gtrsim 6$ through I-band. In summary, we can examine the reionization history by checking whether the high-z GRB afterglows drop out of the NIR filters or not.

In the rest of this subsection, we discuss what is the difference between Cen's scenario and others. To demonstrate the main feature, we assume two schematic reionization histories; (1) single gradual reionization and (2) double sudden reionizations, which are shown in Figure 5 as the solid and dashed curves, respectively. These histories are based on two observational constraints; (1) the neutral fraction of hydrogen $x_{\rm HI} \sim 10^{-5}$ at $z \sim 6$ from the Gunn-Peterson trough found in the $z > 6$ quasars spectra (Becker et al. 2001; White et al. 2003), and (2) the beginning of the reionization is $z \sim 20$ from the large opacity of the electron scattering suggested by *WMAP* (Kogut et al. 2003). For the double reionizations, we also consider different values of $x_{\rm HI}$ in the first reionization epoch.

In Figure 6, we show the expected NIR colors as a function of the source redshift for the afterglow spectrum $f_\nu \propto \nu^{-1/2}$ case (the observing time less than several hours, see Table 3). We find differences between the single and double reionizations in the $I - J$ (panel [a]) and $K - L$ (panel [d]) colors. In panel (a), the GRB afterglows up to $z_{\rm S} \sim 8$ can be seen in both of the I and J bands for the single reionization case, whereas the $I - J$ color of $z_{\rm S} > 7.1$ afterglows diverges in the double reionization case, i.e. the sources drop out of the I-band. This reflects the difference of the increasing rate of the neutral fraction around $z \sim 6$ in two reionization histories. The drop-out redshift in the double reionization case is determined by $\lambda_\beta(1 + z_{\rm S,drop}) = \lambda_\alpha(1 + z_{\rm reion})$, where λ_α and λ_β are the rest-frame wavelength of the Lyα and Lyβ lines, and $z_{\rm reion}$ is the sudden reionization redshift (Haiman & Loeb 1999). In our case, $z_{\rm reion} = 6$. It is worth to noting that the GRB afterglows beyond the drop-out redshift of the I-band ($z_{\rm Ly\alpha,out}^{I} = 6.6$) can be seen through the filter in both of reionization histories.

In panel (d) of Figure 6, we find a significant difference between the two reionization scenarios. While the afterglows beyond the drop-out redshift of the K-band really drop out of the filter for the single reionization, we can

see such afterglows in the twice reionized universe. On the other hand, the afterglows with $z_{\rm S} > 23$ drop out of the K-band even in the double reionization case because the Lyβ break goes out of the filter transmission width, i.e. $\lambda_\beta(1 + z_{\rm S,drop}) = \lambda_{\max}^K[= \lambda_\alpha(1 + z_{{\rm Ly}\alpha,{\rm out}}^K)]$, where $\lambda_{\max}^K$ is the maximum wavelength of the K-band filter. We note here that $z_{\rm reion}(= 20) > z_{{\rm Ly}\alpha,{\rm out}}^K$ in this time, whereas $z_{\rm reion}(= 6) < z_{{\rm Ly}\alpha,{\rm out}}^I$ in the above case.

Any difference between the single and double reionizations cannot be found in the $J - H$ (panel [b]) and the $H - K$ (panel [c]) colors because the neutral fractions in both cases are high enough ($\gtrsim 10^{-4}$) to extinguish the continuum bluer than the Lyα break completely. That is, the GRB afterglows beyond the drop-out redshift cannot be seen in the J and H-bands for both of reionization histories.

Let us summarize how to confirm or refute Cen's scenario: We can conclude that the universe was reionized twice if (1) the GRB afterglows with $z_{\rm S} > z_{{\rm Ly}\alpha,{\rm out}}^K$ is detected in the K-band and (2) the afterglows with $z_{\rm S} > z_{{\rm Ly}\alpha,{\rm out}}^J$ or $z_{\rm S} > z_{{\rm Ly}\alpha,{\rm out}}^H$ drop out of the J or H-bands. However, the null detection of the $z_{\rm S} > z_{{\rm Ly}\alpha,{\rm out}}^K$ GRB afterglows in the K-band does not reject Cen's scenario at once. The null detection only shows the neutral fraction at $z \sim 20$ larger than $\sim 10^{-5}$. In any case, the deep and prompt K-band photometry of the high-z GRB afterglows is useful to examine the ionization state at $z \sim 20$ very much.

6.2. Comment on Lyman break technique

In the above discussions, we assumed that the GRB redshifts are known from other methods. Although the spectroscopy of the optical afterglow or the host galaxies is used to determine the redshift of the low-z GRBs, it may be difficult for the high-z GRBs. The Fe line in the X-ray afterglow (Mészáros & Rees 2003) or some empirical ways using the γ-ray data alone (e.g., Yonetoku et al. 2003) can be useful for the high-z GRBs. In addition, the search for the Lyα break is considered to be useful. Indeed, the spectroscopic detection of the sharp Lyα cut-off (see Figs.2 and 3) is an accurate method to determine the redshift. However, the color selection technique which is often used to find the $z \gtrsim 3$ galaxies (Madau 1995; Steidel et al. 1996) may not be good for the high-z GRBs. This is because the GRB afterglows beyond the drop-out redshift of the considered filter can be detectable if the universe is ionized enough.

For example, if we use $I - J \geq 5$ mag as a criterion to select the high-z GRBs, the selected objects have $z \gtrsim 6.5$ indeed (see Fig.3a and Table 3). However, a number of real $z \gtrsim 6.5$ objects escape the criterion if the neutral fraction is less than $\sim 10^{-5}$. Therefore, we cannot use a simple color selection technique for the high-z GRBs. Spectroscopic observations to detect the Lyα break feature , Fe line (Mészáros & Rees 2003) or empirical methods by using only the γ-ray data (Fenimore & Ramirez-Ruiz 2000; Norris et al. 2000; Ioka & Nakamura 2001; Amati et al. 2002; Atteia 2003; Murakami et al. 2003; Yonetoku et al. 2003) are required.

[6] http://subarutelescope.org/

[7] http://astro.estec.esa.nl/SA-general/Projects/Planck/

6.3. Advantage and disadvantage of NIR colors method

The largest advantage of the NIR color method is its easier availability and higher sensitivity than other methods. The limiting magnitude with a high signal-to-noise ratio of the broad-band NIR photometry reaches much deeper than 20 mag by only a few minute exposure with a 8-m class ground based telescope. For example, the IRCS (Infrared Camera and Spectrograph) equipped with the Subaru telescope (Japanese 8-m class telescope[6]) can reach the 2-σ upper limit of 22 mag by only five minutes exposure in K-band. This magnitude corresponds to $\Delta K \simeq 5$ mag based on the expected L magnitude of $\simeq 16$ mag for the $z \simeq 20$ GRB afterglows at 1 hour after the burst (Fig.4) and $K - L = 1.1$ (Table 3), and also corresponds to the neutral fraction of 3×10^{-6}. Thus, we can put this value as a lower limit of the neutral fraction at $z \sim 20$ for null detection.

A more strict lower limit can be obtained if we detect the emission from the reverse shock (Sari & Piran 1999a,b; Gou et al. 2003). Some GRBs show a very bright early afterglow from the reverse shock. Interestingly, the apparent magnitude becomes ~ 5–6 mag brighter than that shown in Figure 4. In this case, we can reach $\Delta K \simeq 10$ corresponding to $x_{\rm HI} \simeq 6 \times 10^{-6}$. A very early observation is highly desired.

From the detected magnitude or the limiting magnitude for the null detection, the neutral fraction or its lower limit in the corresponding redshift range can be estimated. However, the uncertainty of the obtained neutral fraction may be large if we have only one photometric data. This is because the apparent dispersion of the afterglow luminosities is large. Even in that case, the uncertainty can be controlled in a low level if we use more than two photometric data, i.e. colors, which are independent of the absolute luminosity. This point is one of the important advantages of the NIR color method. Therefore, the NIR multi-colors follow-ups of the GRB afterglows are strongly encouraged.

Miralda-Escudé (1998) and Barkana & Loeb (2003) show that the detailed spectroscopy of the red damping wing of the Lyα break provides us with the optical depth for the line, i.e., the neutral hydrogen column density to the source. However, the spectral resolution required is $\lambda/\Delta\lambda \sim 5000(10^5/\tau_{{\rm Ly}\alpha})$. For a lower opacity, a much higher resolving power is needed. The limiting magnitude for such observations becomes significantly shallow. That is, the method of damping wing measurement do not have sensitivity for a low opacity case. On the other hand, the NIR colors method is practically sensitive against $\tau_{{\rm Ly}\alpha} \lesssim 10$. Therefore, these two methods are complementary each other; if $x_{\rm HI} \sim 10^{-6}$ ($\tau_{{\rm Ly}\alpha} \sim 1$), the NIR colors method becomes very useful, whereas the damping wing method is promising when $x_{\rm HI} \sim 0.1$ ($\tau_{{\rm Ly}\alpha} \sim 10^5$).

Measurement of the CMB polarization anisotropy is also useful. Haiman & Holder (2003) show that we can distinguish how much times the universe is reionized by using EE spectrum with Planck sensitivity in 3σ level. Since the sensitivity of $WMAP$ is not enough, we must await the launch of Planck[7] to reveal the reionization history by the CMB measurement.

Moreover, metal absorption lines like O I λ1302 can be useful to prove the reionization history (Oh 2002; Furlanetto & Loeb 2003). However, the expected equivalent width is very small as $\lesssim 5$ Å. We require the spectroscopy with a resolving power ~ 5000. Unfortunately, observations with a ground-based telescope may be difficult because a huge number of Earth's atmospheric OH lines conceal the metal lines. Only JWST (James Webb Space Telescope)[8] will have such a high spectral resolution among the future space telescopes having the NIR spectrograph. Thus, we need to await its launch to discuss the metal absorption lines.

Technique using the hydrogen 21 cm absorption line is also proposed (e.g., Madau et al. 1997). However, the brightness of GRB afterglows is too faint to use them as a background light source for the present and future radio facilities because the absorption line is very weak (Furlanetto & Loeb 2002). Thus, we need to look for other sources. Although Carilli et al. (2002) proposed luminous high-z radio-loud quasars as a candidate of the background source, it is very uncertain that they exist at $z \sim 20$.

The dispersion measure in GRB radio afterglows may be promising in near future (Ioka 2003; Inoue 2003). If we observe the radio afterglow at about 100 MHz within about 1000 s after the burst occurrence, the delay of the arrival time of the low frequency photons may be detectable by the Square Kilometer Array. As well as the measurement of the red damping wing of the Lyα line, this technique is sensitive to $x_{\mathrm{HI}} \gtrsim 0.1$ (i.e., $\tau_{\mathrm{Ly}\alpha} \gtrsim 10^5$). Thus, this technique and our NIR color method are also complementary each other.

The disadvantage of the NIR color method is the coarse redshift resolution. As discussed in section 4, the neutral fraction obtained by the color method is an averaged one in the redshift range of $z_{\mathrm{Ly}\alpha,\mathrm{in}} \leq z \leq z_{\mathrm{S}}$. Thus, we cannot determine the so-called reionization redshift. Only the redshift range in which the reionization occurred is obtained. However, even such a rough redshift resolution is enough to discuss whether the universe was reionized once, twice, or more.

To know the detailed history of the reionization, the spectroscopy is needed. For this purpose, the Japanese astronomical satellite ASTRO-F[9] can be useful. The satellite will have the spectroscopic sensitivity of ~ 30 μJy around ~ 2 μm, which can detect the GRB afterglows of $z_{\mathrm{S}} \sim 20$ if $x_{\mathrm{HI}} \sim 10^{-6}$ (see Fig.2a). SIRTF (Spece InfraRed Telescope Facility)[10] may not be useful because it has the sensitivity only in the wavelength longer than 5 μm. In future, JWST is much promising. Finally, we note that the narrow-band photometry may be useful because its narrow transmission width provides us with a moderate resolution of redshift keeping a higher sensitivity than that of spectroscopy.

REFERENCES

Amati, L., et al. 2002, A&A, 390, 81
Atteia, J.-L. 2003, A&A, 407, L1
Barkana, R. & Loeb, A. 2003, ApJ, submitted (astro-ph/0305470)
Becker, R. H., et al. 2001, AJ, 122, 2850
Bessell, M. S. 1990, PASP, 102, 1181
Bessell, M. S., & Brett, J. M. 1988, PASP, 100, 1134
Bromm, V., & Loeb, A. 2003, ApJ, 575, 111
Carilli, C. L., Gnedin, N. Y., & Owen, F. 2002, ApJ, 577, 22
Cen, R. 2003a, ApJ, 591, 12
Cen, R. 2003b, ApJ, 591, L5
Chiu, W. A., Fan, X., & Ostriker, J. P. 2003, ApJ, submitted (astro-ph/0304234)
Ciardi, B. & Loeb, A., 2000, ApJ, 540, 687
Ciardi, B., Ferrara, A., & White, S. D. M. 2003, MNRAS, submitted (astro-ph/0302451)
Fenimore, E. E., & Ramirez-Ruiz, E. 2000, astro-ph/0004176
Furlanetto, S. R., & Loeb, A. 2002, ApJ, 579, 1
Furlanetto, S. R., & Loeb, A. 2003, ApJ, 588, 18
Galama, T.J., et al. 1998, Nature, 395, 670
Giavalisco, M., et al. 2003, ApJL, in press (astro-ph/0309065)
Gou, L. J., Mészáros, P., Abel, T., & Zhang, B. 2003, ApJ, submitted (astro-ph/0307489)
Gunn, J. E., & Peterson, B. A. 1965, ApJ, 142, 1633
Haiman, Z., & Loeb, A. 1999, ApJ, 519, 479
Haiman, Z., & Holder, G. P. 2003, ApJ, 595, 1
Hjorth, J. et al., 2003, Nature, 423, 847
Inoue, S. 2003, MNRAS, submitted (astro-ph/0309364)
Ioka, K. 2003, ApJL, submitted (astro-ph/0309200)
Ioka, K., & Nakamura, T. 2001, ApJ, 554, L163
Kogut, A., et al. 2003, ApJ, in press (astro-ph/0302213)
Lamb, D.Q., Reichart, D.E. 2000, ApJ, 536, 1
Leitherer et al. 1999, ApJS, 123, 3
Loeb, A., & Barkana, R. 2001, ARA&A, 39, 19

Madau, P. 1995, ApJ, 441, 18
Madau, P., Meiksin, A., & Rees, M. J. 1997, ApJ, 475, 429
Matheson, T., et al. 2003, ApJ, submitted (astro-ph/0307435).
Mészáros, P. & Rees, M.J. 2003, ApJ, 591, L91
Miralda-Escudé, J. 1998, ApJ, 501, 15
Murakami, T., Yonetoku, D., Izawa, H., & Ioka, K. 2003, PASJ, in press
Nakamoto, T., Umemura, M., & Susa, H. 2001, MNRAS, 321, 593
Nakamura, F., & Umemura, M. 2001, ApJ, 548, 19
Norris, J.P., Marani, G.F., & Bonnell, J.T. 2000, ApJ, 534, 248
Oh, S. P. 2002, MNRAS, 336, 1021
Onken, C. A., & Miralda-Escudé, J. 2003, ApJ, submitted (astro-ph/0307184)
Osterbrock, D. E. 1989, Astrophysics of Gaseous Nebulae and Active Galactic Nuclei (Mill Valley: University Science Books)
Peebles, P. J. E. 1993, Principles of physical cosmology, Princeton University Press, New Jersey
Price, P.A. et al., 2003, Nature, 423, 844
Sari, R., Piran, T., & Narayan, R. 1998, ApJ, 497, L17
Sari, R., & Piran, T. 1999, ApJ, 517, L109
Sari, R., & Piran, T. 1999, ApJ, 520, 641
Sokasian, A., Yoshida, N., Abel, T., Hernquist,L., & Springel, V. 2003, astro-ph/0307451
Somerville, R. S., & Livio, M. 2003, ApJ, 593, 611
Spergel, D., et al. 2003, ApJ, in press (astro-ph/0302209)
Stanek, K. Z., et al. 2003, ApJ, 591, L17
Steidel, C. C., Giavalisco, M., Pettini, M., Dickinson, M., & Adelberger, K. L. 1996, ApJ, 462, L17
Uemura, M. et al. 2003, Nature, 423, 843
White, R. L., Becker, R. H., Fan, X., & Strauss, M. A. 2003, AJ, 126, 1

[8] http://ngst.gsfc.nasa.gov/

[9] http://koala.ir.isas.ac.jp/ASTRO-F/index-e.html

[10] http://sirtf.caltech.edu/

Wiese, W. L., Smith, M. W., & Glennon, B. M. 1966, Atomic
    Transition Probabilities, Vol. 1 (NSRDS-NBS 4; Washington:
    GPO)
Wyithe, J. S. B., & Loeb, A. 2003a, ApJ, 586, 693

Wyithe, J. S. B., & Loeb, A. 2003b, ApJ, 588, L69
Yonetoku, D., Murakami, T., Nakamura, T., Yamazaki, R., Inoue,
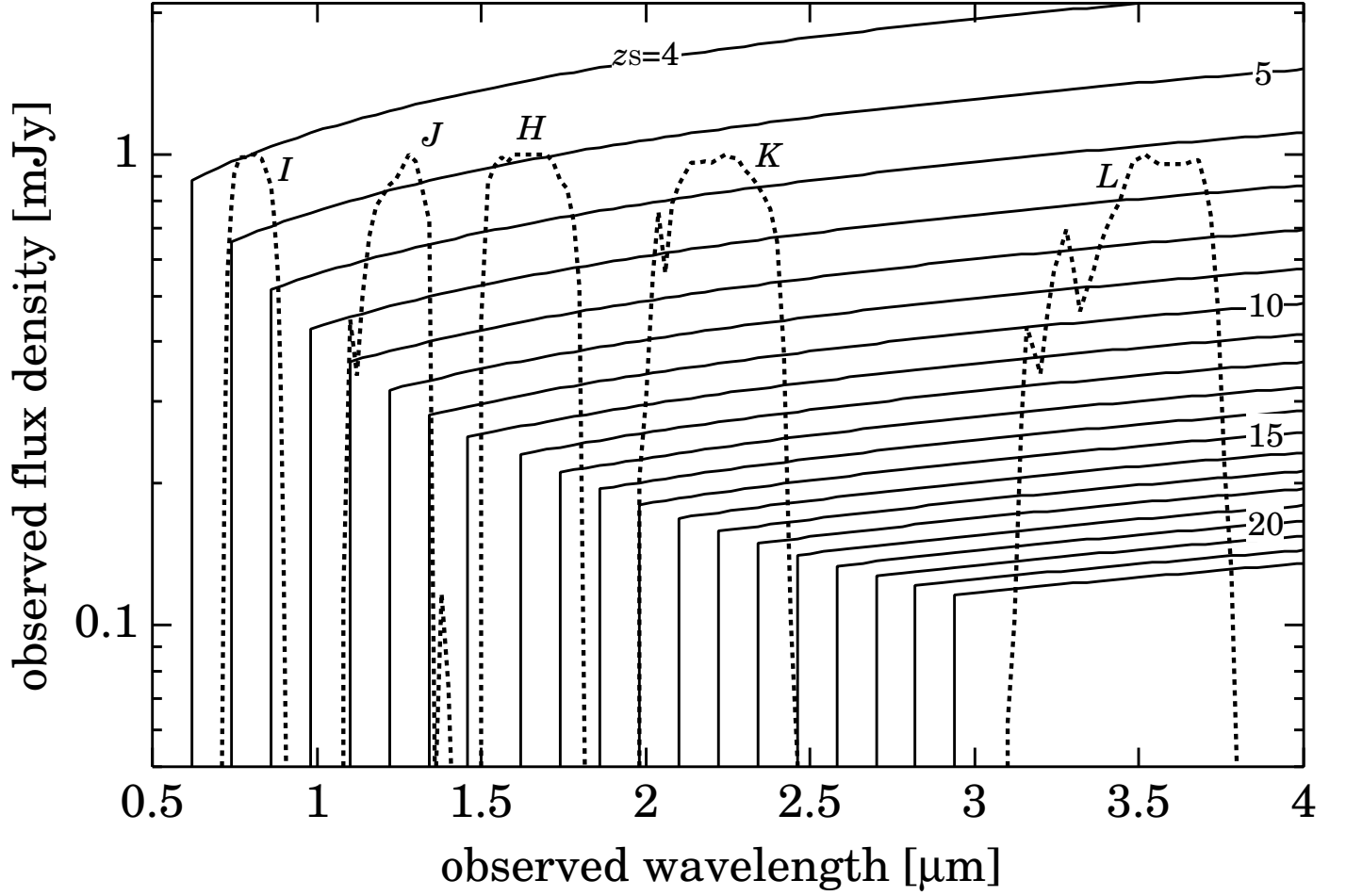   A. K., & Ioka, K. (astro-ph/0309217)

FIG. 1.— Afterglow spectra in the hypothetical neutral universe. The solid curves are the afterglow spectra of the gamma-ray bursts at the redshift $z_S = 4$–23 as indicated in the panel. The observing time is set to be 1 hour after the burst for all curves. The dotted curves are the filter transmissions of I, J, H, K, and L bands (Bessell & Brett 1988; Bessell 1990). These transmission curves are scale free.
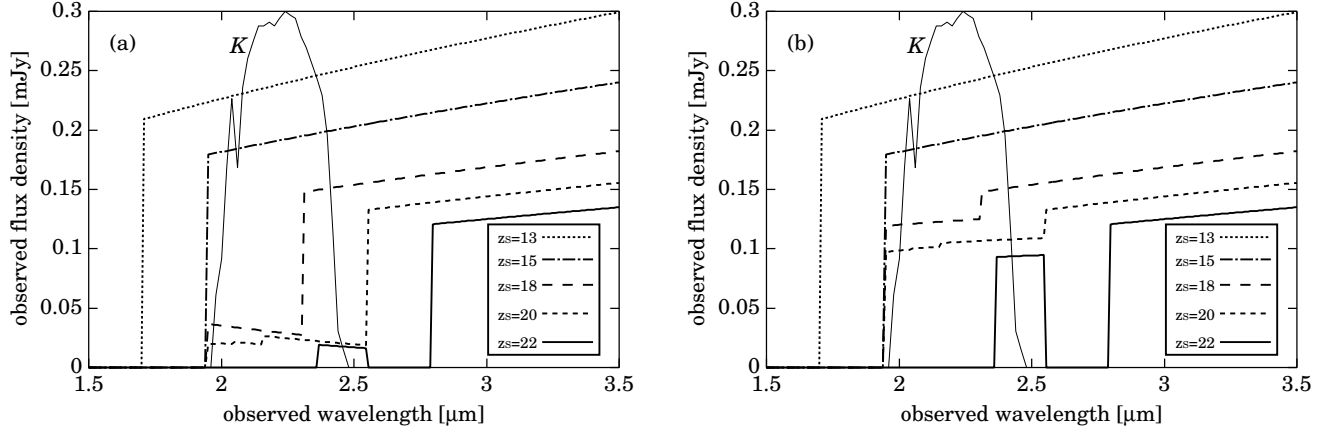

FIG. 2.— Expected near-infrared afterglow spectra of very high redshift gamma-ray bursts. The solid, short-dashed, long-dashed, dot-dashed, and dotted curves are the cases of the source redshift $z_S = 22$, 20, 18, 15, and 13 respectively. The observing time is set to be 1 hour after the burst for all curves. The neutral fraction in $15 \leq z < 20$ is assumed to be 10^{-6} and 10^{-7} for the panels (a) and (b), respectively. The thin solid curve is the filter transmission of K-band (Bessell & Brett 1988). This transmission curve is scale free.
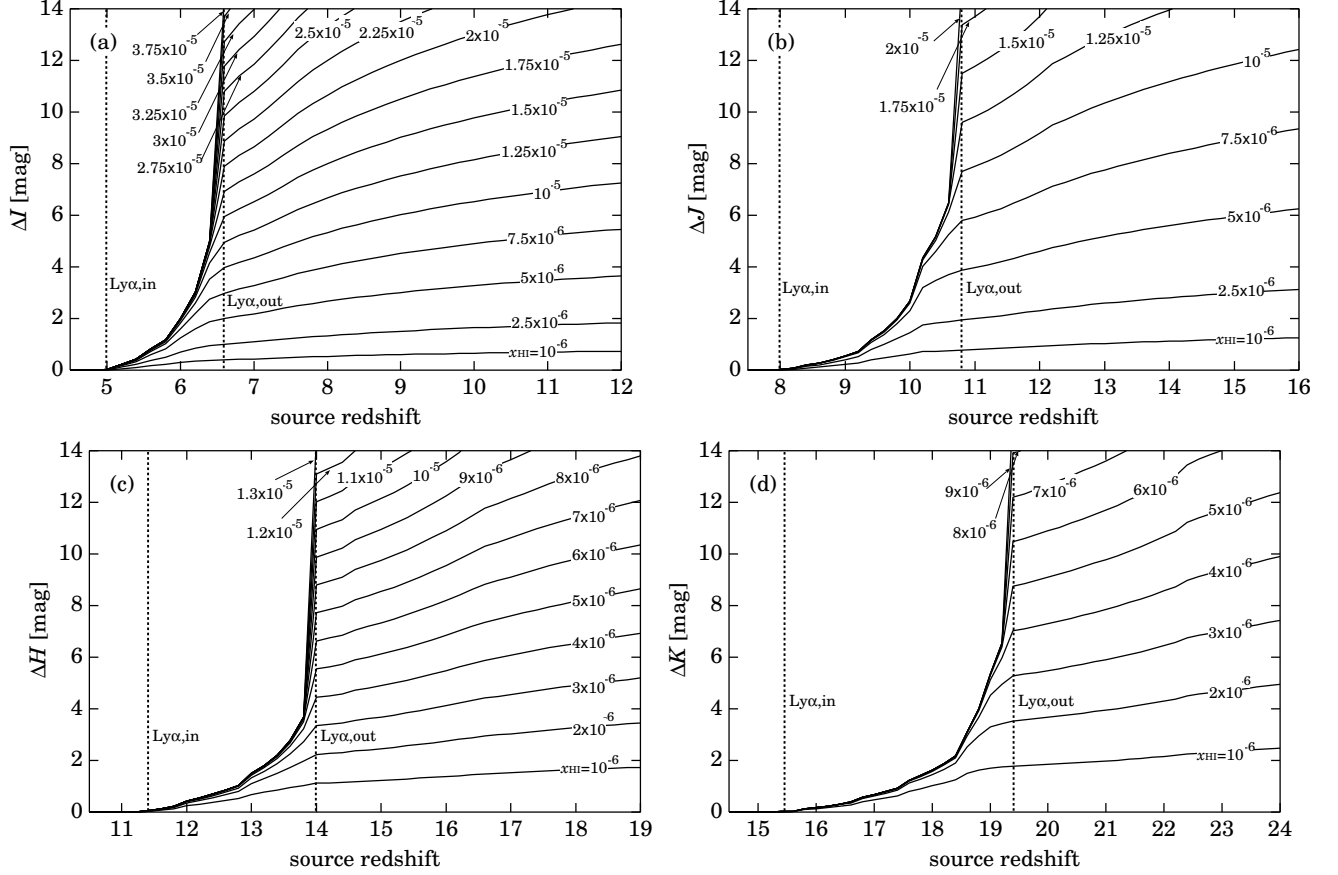
FIG. 3.— The intergalactic absorption in near-infrared bands. The vertical axis in each panel means the absorption amount in each filter (see eq.[11]); (a) I-band, (b) J-band, (c) H-band, and (d) K-band. The solid curves in the panels are loci of the absorption amount as a function of the redshift of the source z_S. The neutral hydrogen fraction, x_{HI}, is assumed to be constant between the redshift when the Lyα break enters the filter transmission and z_S. The assumed x_{HI} is indicated on each curve. Two dotted vertical straight lines in each panel indicate the source redshifts at which the Lyα break enters and goes out of the filter.
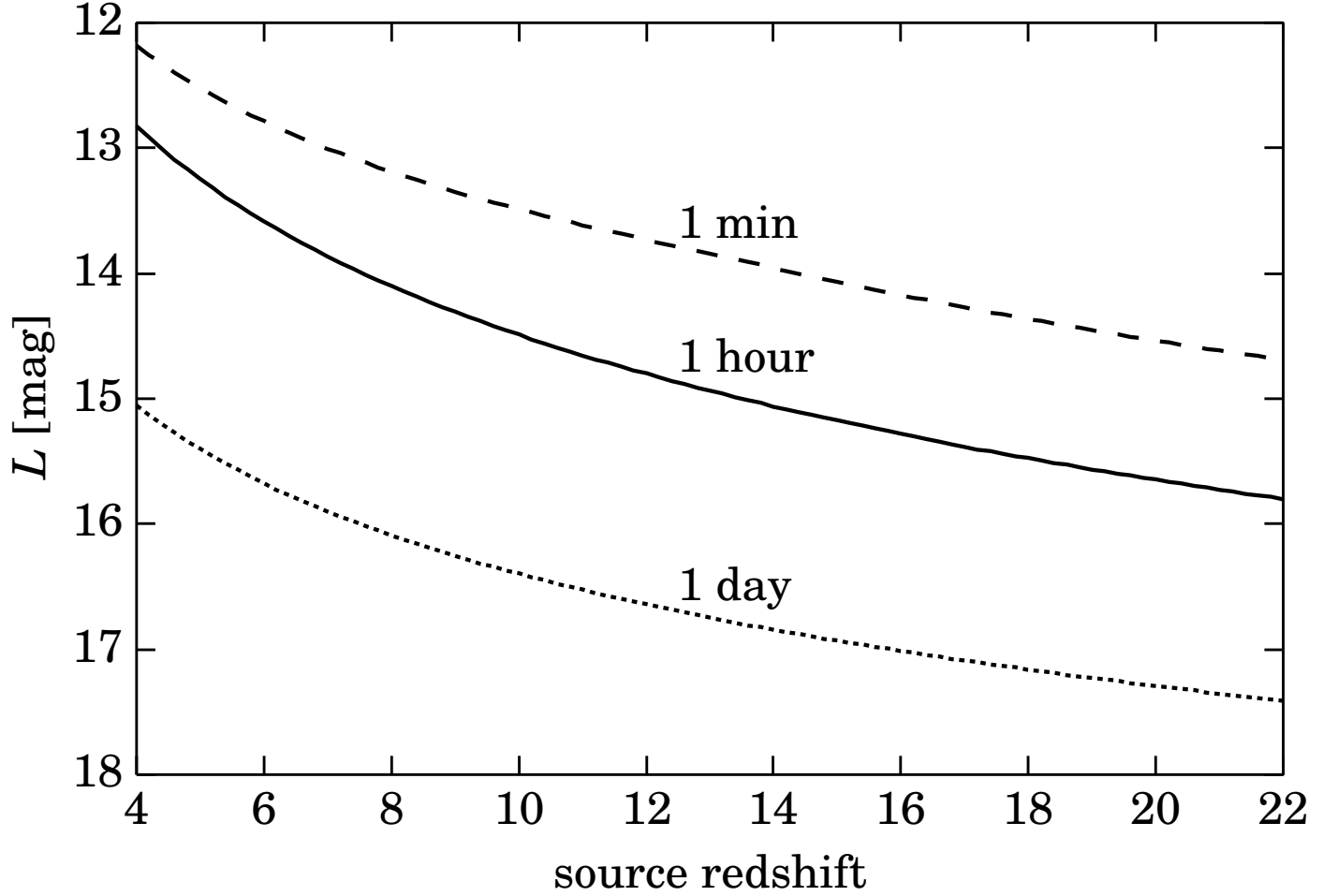
FIG. 4.— The expected apparent magnitude in L-band of the afterglows of the gamma-ray bursts (GRBs) as a function of the source redshift. The dashed, solid, and dotted curves are the cases of 1 minute, 1 hour, and 1 day after the burst occurrence in the observer's frame, respectively. The spectral model of the GRB afterglows by Ciardi & Loeb (2000) is adopted. The assumed parameter set is described in the first paragraph of section 3.
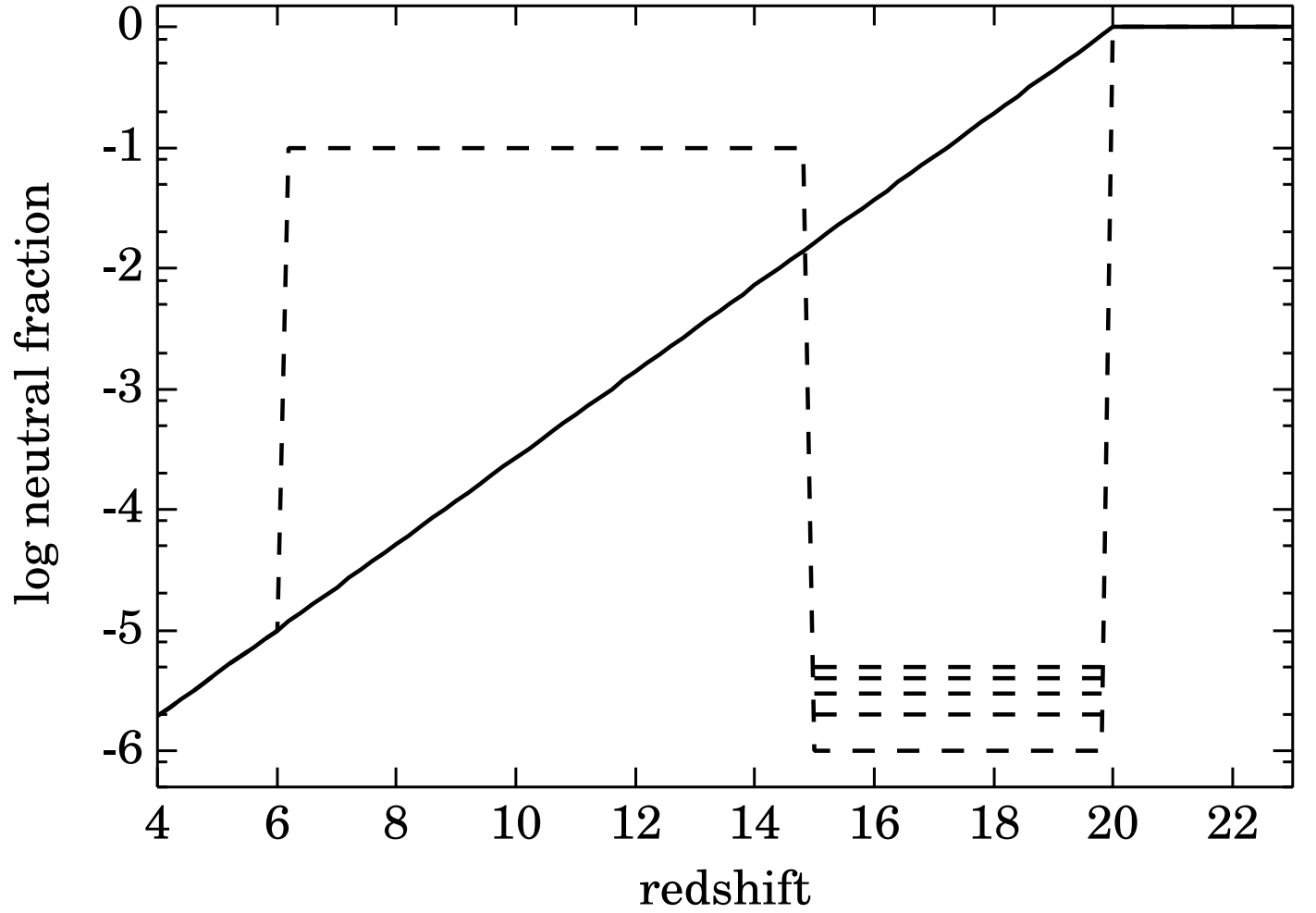
Fig. 5.— Examples of the reionization history. The solid curve is a single gradual reionization case. The dashed curve is a double reionizations case as suggested by Cen (2003a).
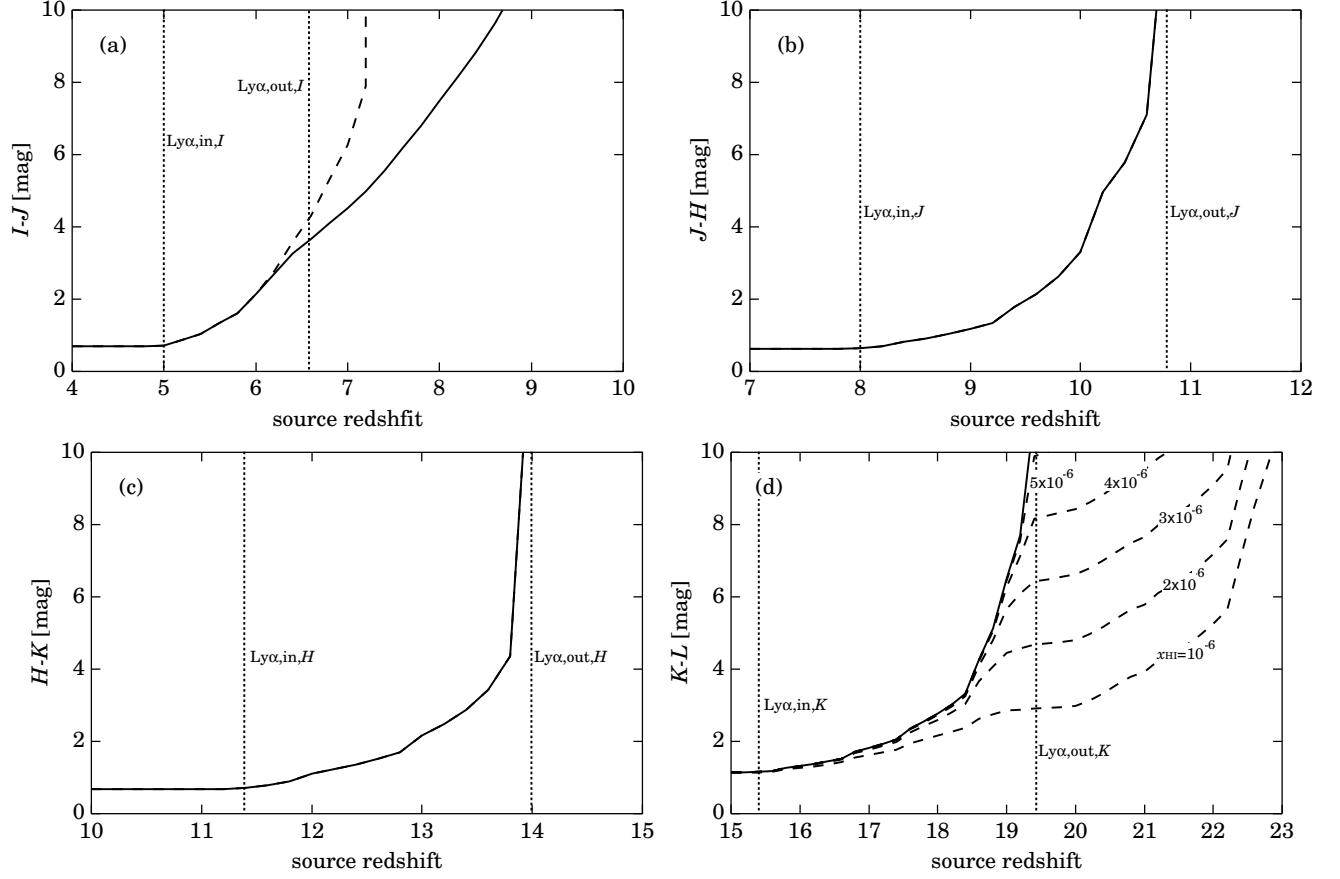
FIG. 6.— Expected near-infrared colors of gamma-ray burst afterglows. (a) $I-J$ colors, (b) $J-H$ colors, (c) $H-K$ colors, and (d) $K-L$ colors. The solid and dashed curves correspond to the cases of the single and double reionizations depicted in Figure 5, respectively. The solid and dashed curves in panels (b) and (c) are perfectly superposed. In panel (d), some cases of the neutral hydrogen fraction in the first reionization are shown. Two dotted vertical straight lines in each panel indicate the source redshifts at which the Lyα break enters and goes out of the indicated filter.

TABLE 1

STAR FORMATION DENSITY REQUIRED TO MAINTAIN $x_{\mathrm{HI}} \sim 10^{-6}$

Stellar mass range $(M_\odot)$	ϵ_{LC} $(10^{61}$ ph $M_\odot{}^{-1})$	ρ_{SFR} $(M_\odot$ yr^{-1} Mpc$^{-3})$
10–100	2	0.05
1–100	0.7	0.1
0.1–100	0.3	0.3

Note. — We calculate the Lyman continuum photon emissivity per unit stellar mass, ϵ_{LC}, by Starburst 99 model (Leitherer et al. 1999) by assuming the Salpeter initial mass function with the tabulated mass range. We also assume the escape fraction $f_{\mathrm{esc}} = 0.1$ and the clumping factor $C = 1$ for the star formation density.

TABLE 2

CHARACTERISTIC REDSHIFTS OF NIR FILTERS

filter	$z_{\mathrm{Ly}\alpha,\mathrm{in}}$	$z_{\mathrm{Ly}\alpha,\mathrm{out}}$
I	5.0	6.6
J	8.0	10.8
H	11.4	14.0
K	15.4	19.4
L	24.6	30.6

Note. — $z_{\mathrm{Ly}\alpha,\mathrm{in}}$ and $z_{\mathrm{Ly}\alpha,\mathrm{out}}$ are the redshifts at which the Lyα break enters and goes out of the filter transmission, respectively.

TABLE 3

NIR AFTERGLOW INTRINSIC COLORS

color	$\propto \nu^{-1/2}$	$\propto \nu^{-p/2}$ $(p = 2.5)$
$I - J$	0.70	1.0
$I - H$	1.3	1.9
$I - K$	2.0	2.8
$I - L$	3.1	4.3
$J - H$	0.62	0.86
$J - K$	1.3	2.8
$J - L$	2.4	3.3
$H - K$	0.67	0.91
$H - L$	1.8	2.4
$K - L$	1.1	1.5

Note. — In the observer's frame, the NIR afterglow spectrum of the GRBs at $z \sim 10$ is proportional to $\nu^{-1/2}$ between ~ 1 minute and several hours after the initial burst and proportional to $\nu^{-p/2}$ for later time.